ACS Biomaterials SCIENCE & ENGINEERING

Article

pubs.acs.org/journal/abseba

Deconstructing HPMCAS: Excipient Design to Tailor Polymer−Drug Interactions for Oral Drug Delivery

Jeffrey M. Ting,[‡] Tushar S. Navale,[†] Seamus D. Jones,[‡] Frank S. Bates,*[,‡] and Theresa M. Reineke*[,†]

[†]Departments of Chemistry and [‡]Department of Chemical Engineering and Materials Science, University of Minnesota, Minneapolis, Minnesota 55455, United States

Supporting Information

ABSTRACT: Spray-dried dispersions (SDDs) are fascinating polymer−drug mixtures that exploit the amorphous state of a drug to dramatically elevate its apparent aqueous solubility above equilibrium. For practical usage in oral delivery, understanding how polymers mechanistically provide physical stability during storage and prevent supersaturated drugs from succumbing to precipitation during dissolution remains a formidable challenge. To this end, we developed a versatile polymeric platform with functional groups analogous to hydroxypropyl methyl cellulose acetate succinate (HPMCAS, a heterogeneous leading excipient candidate for SDDs) and studied its interactions with Biopharmaceutical Classification System Class II drug models probucol, danazol, and phenytoin at various dosages. By conducting reversible addition−fragmentation chain transfer polymerizations with monomeric components chemically analogous to HPMCAS, we synthetically dismantled the highly polydisperse architecture of HPMCAS into well-defined polymer systems (i.e., targetable M_n, $Đ < 1.3$, tunable T_g). In the powdered SDD form, by wide-angle X-ray diffraction all HPMCAS analogs yielded amorphous danazol and phenytoin up to 50 wt % loading, whereas for probucol, hydrophobic methoxy functionality and high polymeric T_g were key to inhibit immediate partitioning into crystalline domains. Nonsink in vitro dissolution tests revealed distinct release profiles. The polymer containing only acetyl and succinoyl substituents spray-dried with probucol increased the area under the dissolution curve by a factor of 180, 112, and 26 over pure drug at 10, 25, and 50 wt % loading, respectively. For crystallization-prone danazol and phenytoin, we observed that the water-soluble polymer with hydroxyl groups inhibited crystal growth and enabled high burst release and supersaturation maintenance. Our findings provide fundamental insight into how excipient microstructures can complex with drugs for excipient formulation applications.

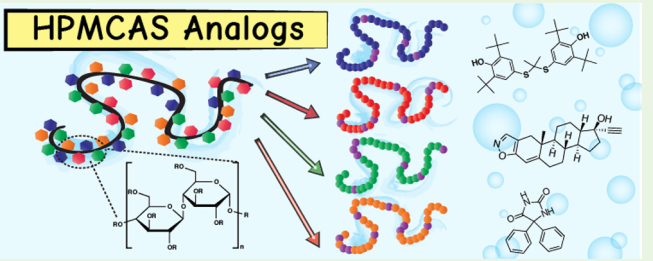

KEYWORDS: *oral drug delivery, amorphous solid dispersions, HPMCAS, polymer-drug interactions, precipitation inhibition*

INTRODUCTION

The prominent rise of high-throughput, target-based screening in biomedical and pharmaceutical research[1,2] has fueled the trajectory of drug discovery advancements over the past decades. However, despite current capabilities of generating vast arrays of new molecular entities (NMEs), federal approval of new drugs remains stagnant to date.[3] In response, many different advanced drug delivery approaches have been developed, often employing imaginative delivery vehicles that integrate key principles in chemistry, engineering, and pharmacology.[4,5] What constitutes the delivery vehicle first depends on the route of delivery. Oral administration remains one of the leading delivery strategies on the market with high patient compliance: in 2013, 46% of 1300 drugs awaiting FDA approval were for oral delivery, more than the reported injection, topical, and inhalation methods combined.[6] This secures oral drug delivery as an attractive avenue to explore new formulations of NMEs as potent drug candidates.

In such formulations, the active pharmaceutical ingredient is one of many components in a tablet. For instance, a single pain-relieving pill containing ibuprofen (a nonsteroidal anti-inflammatory drug) contains 200 mg of the drug agent, which upon weighing constitutes only 60% of the pill by mass. The remaining compounds in a pill are excipients: inactive but crucial ingredients to process formulations and aid in drug delivery to patients with maximum therapeutic efficacy and safety. Unlike the meticulously synthesized small-molecule drugs, excipients are macromolecules that are often polymeric biomaterials. Depending on the application, they can act as fillers, lubricants, binders, coatings, or solubilizers.[7] In particular, because up to 70% of drug candidates in the pharmaceutical pipeline are highly lipophilic, excipients can play a powerful role as solubilizers in oral delivery to overcome poor water solubility in the stomach and gastrointestinal tract, the main bottleneck for oral bioavailability (the fraction of the drug that reaches systemic circulation in the bloodstream).

Many solubilizing strategies have been explored to keep lipophilic drugs in the dissolved state, including lipid-based

Received: June 1, 2015
Accepted: August 26, 2015

DOI: 10.1021/acsbiomaterials.5b00234
ACS Biomater. Sci. Eng. XXXX, XXX, XXX−XXX

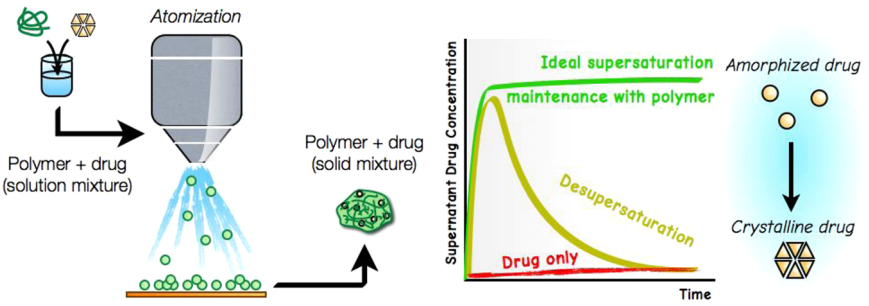

Figure 1. Illustration of the preparation and solubility enhancement mechanism of solid dispersions. Predissolved polymer and drug in solution are atomized with spray drying to form particles containing amorphous drug molecules embedded in a polymer matrix. Upon oral administration, polymers ideally aim to kinetically inhibit drug precipitation at high supersaturation levels for gastrointestinal absorption (6−8 h).

Scheme 1. Chemical Structures of (A) HPMCAS with Its Heterogeneous Pendant Functional Groups, (B) Binary Copolymers Prepared with RAFT Chemistry,[a] and (C) Protected/Deprotected Glycopolymers[b]

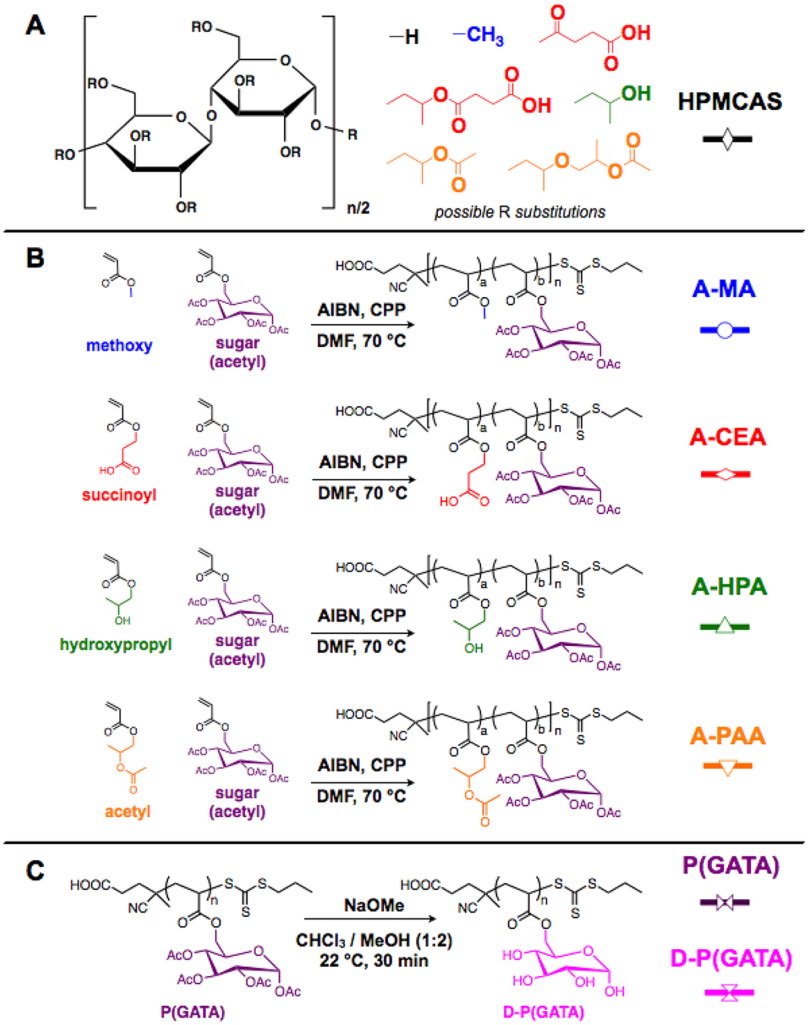

[a]Here, the initiator and chain transfer agent were AIBN (2,2′-azobis(2-methylpropionitrile)) and CPP (4-cyano-4-(propylsulfanylthiocarbonyl)-sulfanylpentanoic acid), respectively. CPP was synthesized according to the work of Xu et al.[14] [b]P(GATA) was first synthesized with identical RAFT conditions, as described in our previous work.[15]

approaches,[8] particle-size reduction,[9] and amorphization.[10] Of these various approaches, solid dispersions have gained significant interest due to their potential to raise the apparent solubility of a drug by orders of magnitude above its equilibrium level.[11] This is accomplished by trapping drug molecules in an amorphous state within a polymer matrix through processes such as spray drying, where polymer−drug solutions are atomized with a heated gas stream (Figure 1). This unit operation is established in industrial settings and scalable to kilogram amounts of material. Upon oral administration, solid dispersions aim to address the limited bioavailability of drugs, where the polymer enables rapid drug

DOI: 10.1021/acsbiomaterials.5b00234
ACS Biomater. Sci. Eng. XXXX, XXX, XXX−XXX

dissolution and generates supersaturation for enhancing intestinal absorption during its residence time (shown graphically in Figure 1). The primary role of the polymer in solid dispersions is to (i) stabilize amorphous drug molecules from recrystallization in the solid-state and (ii) facilitate supersaturation maintenance in the solution-state upon dissolution.

Among the many synthetic and natural polymers used for solid dispersions, hydroxypropyl methyl cellulose acetate succinate (HPMCAS, shown in Scheme 1) has been identified as a leading excipient for many different drug molecules. In particular, prior work conducted by Friesen et al.[12] and Curatolo et al.[13] have demonstrated its exceptional solubilizing performance compared to a library of common polymer excipients. However, despite its incredible effectiveness as a precipitation inhibitor, ill-defined structural variables (i.e., polydisperse molecular weight, heterogeneous chemical substitution, intramolecular cross-linking) severely limit HPMCAS for mechanistic studies. To elucidate some of the underlying molecular interactions of HPMCAS, we used reversible addition−fragmentation chain transfer (RAFT) polymerization to prepare well-defined copolymer analogs (Scheme 1), containing an acrylic monomer that correspond to a chemical moiety in HPMCAS (either methoxy, hydroxypropyl, acetyl, or succinoyl) and a glycomonomer (glucose-6-acrylate-1,2,3,4-tetraacetate, or GATA). Additionally, GATA homopolymers in the sugar-protected and sugar-deprotected form were synthesized as comparisons (screening attempts of similar selective hydrolysis and its shortcomings for the two-component systems are detailed in the Supporting Information). Herein, color schemes will be consistently used to denote the monomeric component in reference to HPMCAS. Furthermore, Scheme 1 shows the colored nomenclature and symbols of each excipient used in the dissolution plots for reference.

After preparing these two-component HPMCAS analogs, we selected model drugs to spray dry into solid dispersions. Among the immense pool of NMEs in the drug discovery stage, up to 60% are categorized as Biopharmaceutical Classification System (BCS) Class II materials, or drugs with high systemic permeability but low solubility for oral administration.[16] Among the many physiochemical properties available to categorize these NMEs, we view that they can be distinguished by their log P and melting temperature (T_m) values, representing measures of precipitation from solution by solid−liquid phase separation and crystallization, respectively. Thus, we chose three BCS Class II model drugs to span the log P−T_m state space: probucol (antihyperlipidemic), danazol (antiestrogenic), and phenytoin (antiepileptic). Figure 2 shows the log P−T_m location and chemical structure of these model drugs.

This work presents a systematic approach to identify underlying functions of the chemical groups in HPMCAS and to advance rational excipient formulation principles in oral drug delivery. In this manner, we spray-dried these well-defined polymers with probucol, danazol, and phenytoin as a function of drug loading and characterized the resultant solid- and solution-state properties in vitro. By studying how specific chemical functional groups in polymers impart desirable noncovalent polymer−drug interactions, we work toward establishing fundamental structure−property relationships that can be universally extended toward the development of more sophisticated biomaterials, controlled drug delivery strategies, and advanced bionanotechnology applications.

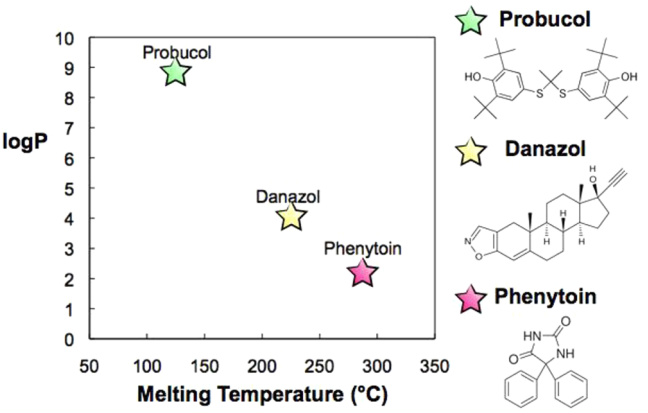

Figure 2. BCS Class II model drugs probucol, danazol, and phenytoin in the log P−melting temperature state space. Chemical structures of the drugs are shown to the right.

RESULTS AND DISCUSSION

Polymer Synthesis and Molecular Characterization. With a combination of reactivity ratio studies and predictive modeling, we have previously demonstrated the ability to generate heteropolymers (multicomponent statistical polymers) with precise structural variables and chemical functionalities akin to HPMCAS.[17] This approach has motivated interesting multimonomer sequencing characterization techniques[18] and enabled us to prepare a tunable five-component system with RAFT polymerization mimicking HPMCAS.[15] In general, this technique allows a facile route to uniform polymers in terms of length (molecular weight) and monomeric incorporation. Such control allowed us to explore cohesive polymer−drug interactions by varying system parameters, e.g., polymer amphiphilicity, ionization at gastrointestinal pH levels, hydrogen bonding capability, etc. As illustrated in Scheme 1, we synthesized binary copolymers to isolate and better understand the role of HPMCAS functional groups in solid dispersions. The Mayo−Lewis[19] and Skeist[20] models were used with measured reactivity ratios to predict the chemical incorporation of monomers. Using these models, we showed that statistical placement of glycomonomer GATA was expected for all systems with little compositional drift effects even at high monomer conversions (see the Supporting Information).

Polymer Characterization Results. Table 1 summarizes the physical properties of our statistical acrylic polymers containing the corresponding groups of HPMCAS: A-MA (methoxy), A-CEA (succinate), A-HPA (hydroxypropyl), A-PAA (acetate), P(GATA) (acetate), and D-P(GATA) (hydroxyl). Compositions of the copolymers were selected (1) to have equivalent targeted molecular weights and (2) vary the glass transition temperature (T_g). To this end, RAFT polymerizations of A-MA, A-CEA, A-HPA, and A-PAA were conducted with a degree of polymerization of 305, 170, 190, and 175, respectively, to near completion. Representative ^{1}H NMR spectra of the polymers to calculate the chemical composition are provided in the Figure S2. The absolute number-average molecular weight (M_n) was measured by size-exclusion chromatography (SEC, representative traces in the Supporting Information), and the dispersity ($Đ$) of the molecular weight distribution from SEC was low for all systems, demonstrating the controllable utility of RAFT chemistry in producing well-defined excipients.

DOI: 10.1021/acsbiomaterials.5b00234
ACS Biomater. Sci. Eng. XXXX, XXX, XXX−XXX

Table 1. Molecular Characterization of Prepared Polymer Systems

system	polymer comp. (mol %)[a](MA/CEA/HPA/PAA/GATA)	T_g[b] (°C)	dn/dc[c] (mL/mg)	M_n[d] (kg/mol)	$Đ$[e]	visual sol.[f]
A-MA	84/0/0/0/0/16	51	0.0724	40.1	1.22	insoluble
A-CEA	0/86/0/0/0/14	60	0.0815	39.2	1.24	soluble
A-HPA	0/0/86/0/0/14	49	0.0656	40.1	1.12	insoluble
A-PAA	0/0/0/0/77/23	15	0.0627	44.1	1.10	insoluble
P(GATA)	0/0/0/0/0/100	111	0.0844	25.8	1.04	insoluble
D-P(GATA)	0/0/0/0/0/100	124	[g]	[g]	[g]	soluble

[a]Molar polymer composition, determined from ^{1}H NMR of the purified polymer. [b]Glass transition temperature, measured by differential scanning calorimetry. [c]Differential refractive index, determined by refractometry in SEC-grade tetrahydrofuran (THF) at 25 °C (see Figure S4). [d]Measured M_n, determined from SEC using THF as the elutant at 25 °C and measured dn/dc values. [e]Dispersity = M_w/M_n, determined from SEC. [f]Relative visual solubility at 9 mg/mL (dissolution conditions for 10 wt % SDDs) in a solution of phosphate buffer saline (pH 6.5) with 0.5 wt % fasted simulated intestinal fluid powder at 37 °C. [g]Insoluble in THF.

Table 2. Drug Physicochemical Properties

drug	log P[a]	T_g[b] (°C)	T_m[c] (°C)	pred. sol.[d] (μg/mL)	PBS sol.[e] (μg/mL)	mol. wt.[f] (g/mol)	pK_a[g]
probucol	8.92	24.9	125	0.0418	4.0	517	10.29
danazol	3.62	N/A[h]	226	17.6	26.1	338	17.59
phenytoin	2.26	N/A[h]	286	71.1	47.8	252	9.47

[a]Calculated octanol/water partition coefficient value.[24] [b]Measured glass transition temperature by second-heating differential scanning calorimetry. [c]Melting temperature. [d]Predicted solubility in water at 25 °C.[24] [e]Measured solubility in phosphate buffer saline (pH 6.5) solution with 0.5 wt % fasted simulated intestinal fluid powder at 37 °C after 6 h. [f]Molecular weight. [g]Predicted acid dissociation constant.[24] [h]Not experimentally measurable by DSC because of the fast crystallization of the drug.

The inclusion of monomer GATA (synthesized according to the procedure reported by Mahkam and co-workers[21]) elevated the T_g of all binary systems by differential scanning calorimetry (DSC), compared to the homopolymers (P(MA), P(CEA), P(HPA), and P(PAA) (DSC analysis is provided in the Supporting Information). Babcock et al. recommended a criteria of T_g > 50 °C to impede crystallization for shelf life.[22] To illustrate the importance of T_g in excipient design, the acetyl analog A-PAA was synthesized with a low T_g value (15 °C). GATA was homopolymerized under the same RAFT conditions for a high-T_g acetyl system. Furthermore, P(GATA) was deprotected with high fidelity using sodium methoxide under basic conditions as a water-soluble hydroxyl system. In a well-mixed aqueous setting at 37 °C, A-CEA and D-P(GATA) were relatively water-soluble, while A-MA, A-HPA, A-PAA, and P(GATA) were insoluble.

Polymer Precipitation Inhibition Screening. Because A-CEA and D-P(GATA) were visually soluble in the dissolution media (phosphate buffer saline, PBS at pH 6.5, with 0.5 wt % fasted simulated intestinal fluid powder, FaSSIF), we tried to gauge their precipitation inhibition ability for probucol, danazol, and phenytoin. These drugs' physiochemical properties are summarized in Table 2. From the log P, T_m, and solubility data, these drugs exhibit poor water solubility. As seen in the representative polarized light microscopy images in Figure 3, when they are introduced at supersaturation (1000 μg/mL) into PBS at 37 °C via solvent shift, precipitation was quickly observed in the absence of polymeric excipient. The more-lipophilic probucol underwent immediate phase separation, whereas small birefringent crystallites of danazol and phenytoin were detected after 10 min.

When predissolved A-CEA or D-P(GATA) was present at identical supersaturation conditions, precipitation was either dramatically reduced or suppressed for the following hour (Figure 3). It should be noted that because this type of study is drug concentration-dependent and does not fully capture the dynamics of solid dispersion dissolution, these experiments simply served as a qualitative screening tool to examine how drugs precipitate out of solution and the overall supersaturation maintenance capability of polymers. More rigorous investigations into solid−liquid/liquid−liquid phase separation, nucleation, and crystal growth are underway.

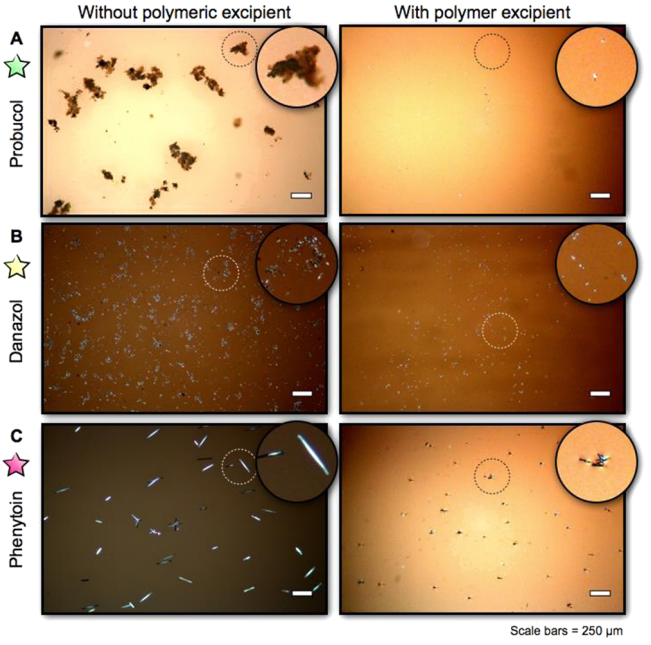

Figure 3. Bright-field polarized light microscopy (PLM) images of (A) probucol, (B) danazol, and (C) phenytoin in the absence (left) and presence (right) of select predissolved polymer (A-CEA for probucol, D-P(GATA) for danazol, and D-P(GATA) for phenytoin at 9000 μg/mL) after 10 min in filtered PBS buffer solution at 25 °C. Drugs (1000 μg/mL) were introduced via a solvent shift method with 2 vol % DMSO. Scale bars of PLM images denote 250 μm. Circular insets of a select region show a 3× magnification with the diameter representing 340 μm.

Preparation and Characterization of Spray-dried Dispersions (SDDs). We spray-dried our six acrylic polymer

DOI: 10.1021/acsbiomaterials.5b00234
ACS Biomater. Sci. Eng. XXXX, XXX, XXX−XXX

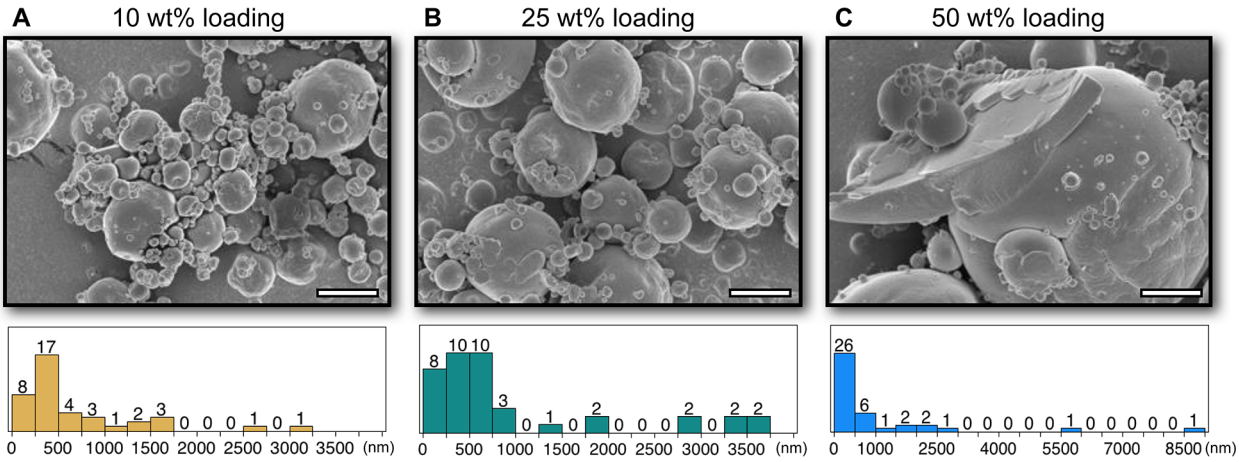

Figure 4. Representative scanning electron microscopy (SEM) images and size distribution of A-CEA polymer with danazol at (A) 10 wt % loading, (B) 25 wt % loading, and (C) 50 wt % loading. Scale bars in SEM images denote 2 μm.

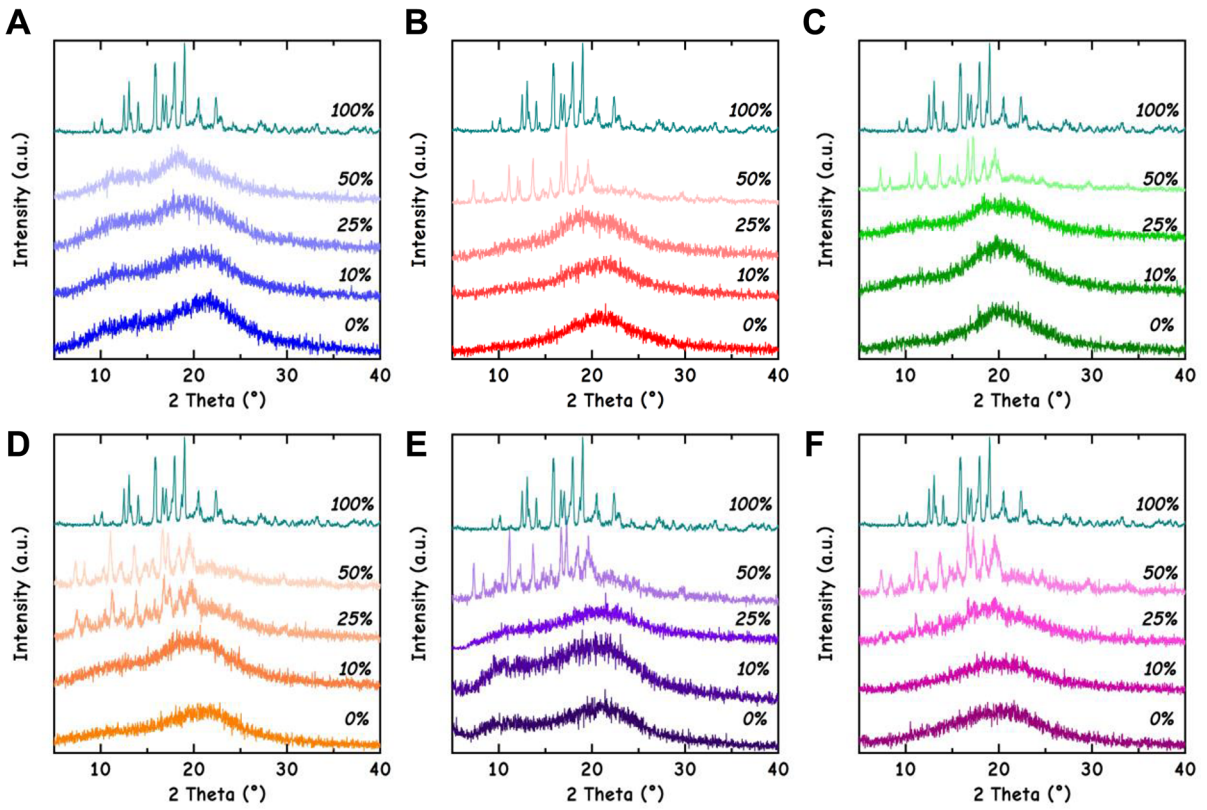

Figure 5. Powder X-ray diffraction (PXRD) patterns of (A) A-MA, (B) A-CEA, (C) A-HPA, (D) A-PAA, (E) P(GATA), and (F) D-P(GATA) at 10, 25, and 50 wt % probucol loading with only spray-dried polymer (0%) and neat probucol (100%). PXRD curves at each level of drug loading were vertically shifted.

systems with BCS Class II drugs probucol, danazol, and phenytoin at 10, 25, and 50 wt % drug loading. To predissolve the polymer and drug mixtures, we used acetone for probucol and phenytoin experiments, and methanol for danazol. All spray drying experiments except for A-PAA had 70−90% yield of SDDs by mass−transfer of powdery particles from the filter paper resulted in minor sample loss. For A-PAA SDDs, less than 50% material was recovered from a yellow semiplasticized film residue on the filter paper with residue on the spray dryer column walls. We attribute this to the low T_g of the polymer, illustrating the importance of selecting a high T_g excipient for glass stabilization.[23] Regardless, by thermogravimetric analysis, prepared SDDs exhibited <1 wt % residual solvent (see the Supporting Information).

SDD Particle Morphology. We employed several solid-state characterization techniques to examine the particles. Representative scanning electron microscopy (SEM) images of A-CEA spray-dried with danazol are shown in Figure 4. A range of 5- to 10-fold reduction in particle size from neat danazol (see the Supporting Information) is evident in prepared SDDs. All particles were generally spherical and polydisperse in terms of geometric diameter. This was a direct consequence of the atomization and drying processes of a lab-scale spray dryer.[25] The microparticle solidification was likely driven by a solute

DOI: 10.1021/acsbiomaterials.5b00234
ACS Biomater. Sci. Eng. XXXX, XXX, XXX−XXX

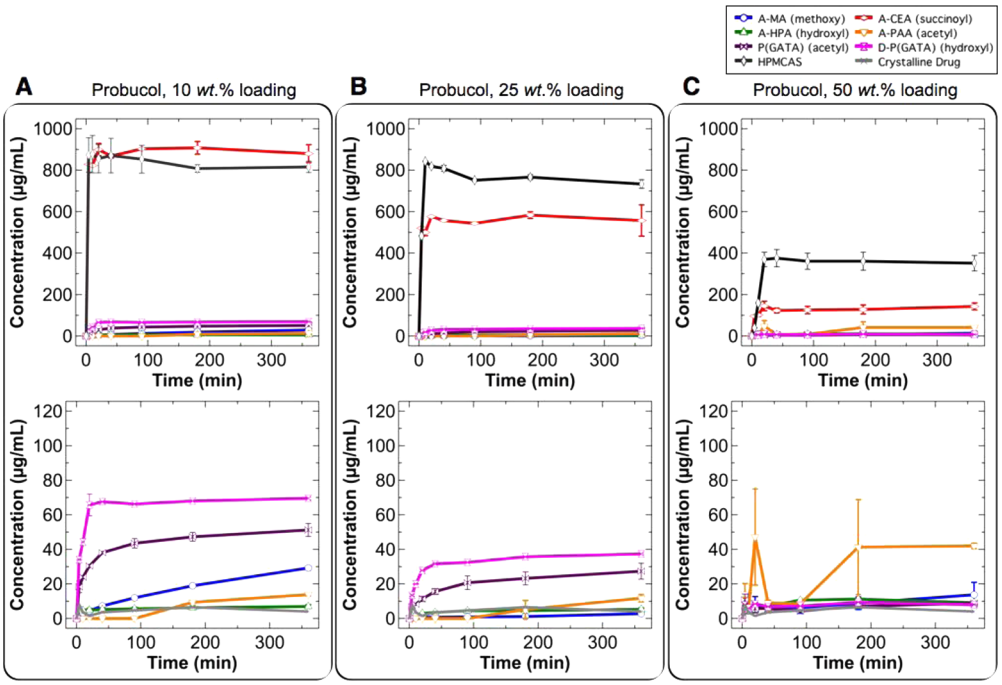

Figure 6. Dissolution tests of probucol-loaded systems with A-MA (blue circle), A-CEA (red diamond), A-HPA (green triangle), A-PAA (orange inverted triangle), P(GATA) (purple bowtie), D-P(GATA) (pink hourglass), and HPMCAS (black rhombus) at (A) 10 wt % loading, (B) 25 wt % loading, and (C) 50 wt % loading. The dissolution of crystalline drug (gray X) is also shown as a reference. The total drug loading of all experiments is 1000 μg/mL. The top and bottom rows show the full and up-close dissolution profiles, respectively. Error bars denote the range of the measured data.

surface enrichment and shell-skin formation mechanism,[23] where solid sphere morphology is obtained from an immediate, rigid shell formation. Molecules with fast crystallization kinetics may phase separate or be induced into polymer- and drug-rich regions. As drug to polymer ratio increased, larger particles were observed, and the particle size distribution broadened. Nonspherical, irregular structures at 50 wt % loading supported the formation of phase-separated drug-rich domains. Such features compromise not only the shelf life of a drug but also its dissolution performance by acting as heterogeneous nucleation points. This illustrates the trade-off between drug loading and efficacy in preparing amorphous solid dispersions.

SDD Particle Amorphicity. Next, to examine the amorphicity of the prepared SDDs as a function of drug loadings, powder X-ray diffraction (PXRD) experiments were conducted. With this technique, crystalline drug lattices can be detected in the form of sharp peaks in the one-dimensional diffraction pattern. For all danazol and phenytoin systems, no crystals were detected in the SDDs (Supporting Information). Figure 5 shows the PXRD patterns for all excipient systems with probucol. Within the resolution of the technique, A-MA best maintains probucol in the amorphous form, where no drug crystals are detected up to 50 wt % loading (Figure 5A).

For all other systems, sharp crystalline peaks are evident at 50 wt % probucol loading. The polymorphism of probucol in two forms is well-documented in the literature[26] and accounts for the minor peak misalignment compared to neat probucol. Only A-PAA exhibits crystallinity at 25 wt % loading (Figure 5D), a direct consequence of the polymer's low T_g and inability to hinder molecular mobility. In contrast, P(GATA) (which contains the same acetate functionalities but has a significantly higher T_g) appears amorphous at 25 wt % loading. Thus, we verify that T_g is an important process parameter to kinetically inhibit the molecular mobility of a drug. Additionally, we analyzed the prepared SDDs with modulated differential scanning calorimetry (MDSC) and Fourier transform infrared (FTIR) spectroscopy to assess polymer−drug miscibility and interactions (see the Supporting Information for representative plots). All SDDs at all drug loadings exhibited a single T_g, indicative of good homogeneity to a first approximation. By FTIR, as the ratio of polymer to drug increased in the SDD samples, the O−H stretching absorption in neat probucol and danazol were shifted and broadened, indicative of hydrogen bonding; SDDs containing phenytoin did not give conclusive results. Rumondor et al. have also reported similar observations for probucol and other drugs.[27] In general, the pre-existing solid state of SDDs is of great importance to dissolution and supersaturation maintenance. Investigation into the effects of temperature and moisture on the shelf life of these HPMCAS-based systems is currently underway. We anticipate interesting comparisons to studies such as moisture-induced phase separation analysis[28] for solid dispersions.

Biorelevant In Vitro Dissolution Testing. In general, in vitro drug release experiments are conventionally performed using United States Pharmacopeia (USP) apparatuses, in which parameters such as formulation disintegration or drug release rates can be measured under sink conditions. While these compendial USP dissolution tests provide meaningful standardized metrics for drug formulation, important phenomenological factors like periodic gastric emptying are not fully captured. Gao and Shi have provided a comprehensive discussion of novel noncompendial strategies to complement USP dissolution tests.[29] Moreover, due to the metastable nature of solid dispersions and the central role of polymers to kinetically hinder precipitation, developing more meaningful physiologically relevant dissolution tests to reflect in vivo

DOI: 10.1021/acsbiomaterials.5b00234
ACS Biomater. Sci. Eng. XXXX, XXX, XXX−XXX

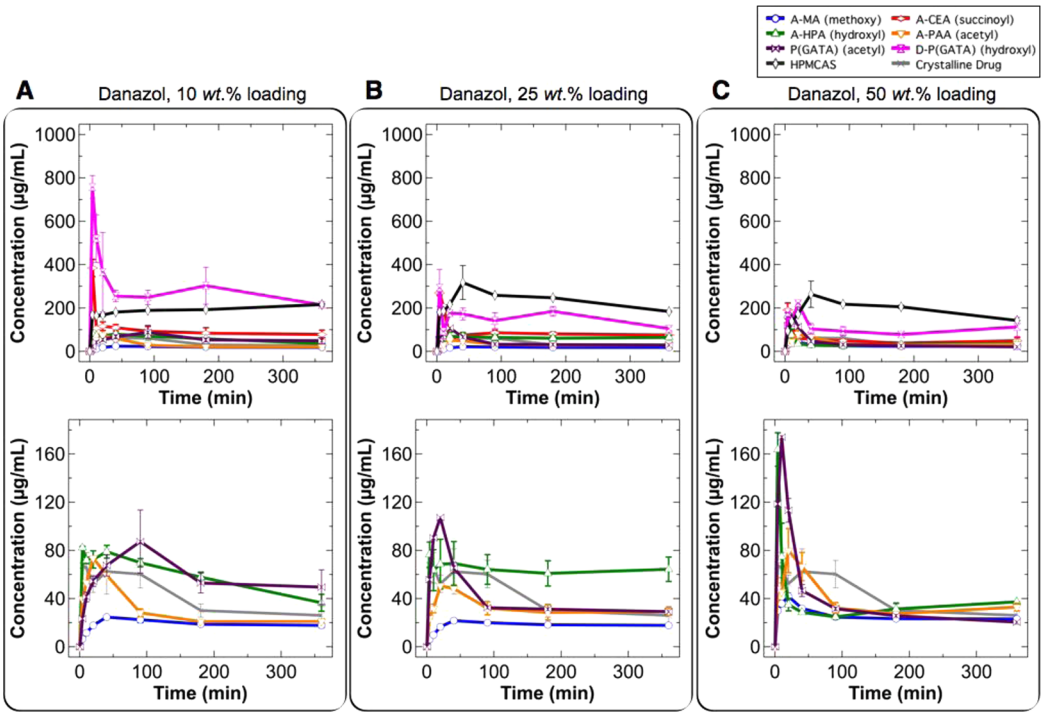

Figure 7. Dissolution tests of danazol-loaded systems with A-MA (blue circle), A-CEA (red diamond), A-HPA (green triangle), A-PAA (orange inverted triangle), P(GATA) (purple bowtie), D-P(GATA) (pink hourglass), and HPMCAS (black rhombus) at (A) 10 wt % loading, (B) 25 wt % loading, and (C) 50 wt % loading. The dissolution of crystalline drug (gray X) is also shown as a reference. The total drug loading of all experiments is 1000 μg/mL. The top and bottom rows show the full and up-close dissolution profiles, respectively. Error bars denote the range of the measured data.

supersaturated states remains critical to clinical administration. Regardless, Higashino et al. have studied the in vitro-in vivo correlation for supersaturated BCS Class II drugs under nonsink conditions and corresponding oral absorption in rats; for drugs that do not undergo significant first-pass metabolism, they demonstrated good agreement between in vitro dissolution/precipitation profiles and measured dosages absorbed from the intestine.[30]

We performed nonsink microcentrifuge dissolution testing to monitor the apparent concentration of supersaturated drug in the supernatant, assumed to be solubilized in either the molecularly dissolved or colloidal aggregates state, and resultantly bioavailable for oral absorption. This dissolution procedure is identical to work conducted by Friesen and co-workers, who were one of the first to identify HPMCAS as a leading excipient for a library of poorly water-soluble drugs.[12] Colloidal aggregates here are defined as materials smaller than 1−200 nm (the supernatant of centrifuged samples were examined for precipitated solids by polarized light microscopy). All dissolution tests were conducted with a total targeted drug concentration (C_{tot}) of 1000 μg/mL in biorelevant medium (PBS solution at 37 °C with 0.5 wt % FaSSIF). Aliquots were taken periodically after centrifugation (16 100 × g for 1 min, where g is Earth's gravitational acceleration) to settle precipitated solids and diluted with methanol for reverse-phase high-performance liquid chromatography (HPLC) analysis. Tabulated maximum attained drug concentration (C_{max}) and drug concentration at 360 min ($C_{360\ min}$) values are provided in the Supporting Information.

Herein, dissolution experiments for all polymer−drug combinations and drug dosages will be presented, and observations in the concentration−time curves for each individual drug will be discussed. A summary of the apparent solubility enhancement will then be shown with a general outlook on excipient design. These trends elucidate mechanistic details surrounding HPMCAS as an excipient for solid dispersions.

Probucol Dissolution. The dissolution performance of probucol-containing systems in Figure 6 is consistent with our previous findings with five-component HPMCAS analogs.[15] The best-performer polymer A-CEA ionizes (pK_a of succinoyl groups ∼5) and swells immediately in the aqueous (pH 6.5) environment to form a visually clear solution, enabling the quick release and supersaturation maintenance of probucol in less than 10 min at all drug loadings. The rapid polymer solvation accelerates chain detachment, and thus, the rate of drug release is closely associated with the dissolution of A-CEA. Colloidal polymer complexation with probucol is able to maintain drug concentration by several orders of magnitude over crystalline probucol's saturation concentration (∼5 μg/mL). The C_{max} dramatically decreases as a function of increasing drug dosage (approximately 910 to 580 to 145 μg/mL) because of decreased stabilizing polymer.

Qualitatively, A-CEA behaves similarly to HPMCAS for probucol, indicating that the opposing balance between hydrophobicity (acetyl) and ionization (succinoyl) is critical to suppressing solid−liquid phase separation. Schram and co-workers used atomic force microscopy to demonstrate how HPMCAS conformationally expands due to charge repulsion at gastrointestinal pH levels and inhibits drug crystal growth by blocking growth sites.[31] We believe that the similarity in dissolution between A-CEA and HPMCAS SDDs indicates that an analogous mechanism is responsible for solubilizing probucol: at pH 6.5 ionized succinoyl groups enable rapid

DOI: 10.1021/acsbiomaterials.5b00234
ACS Biomater. Sci. Eng. XXXX, XXX, XXX−XXX

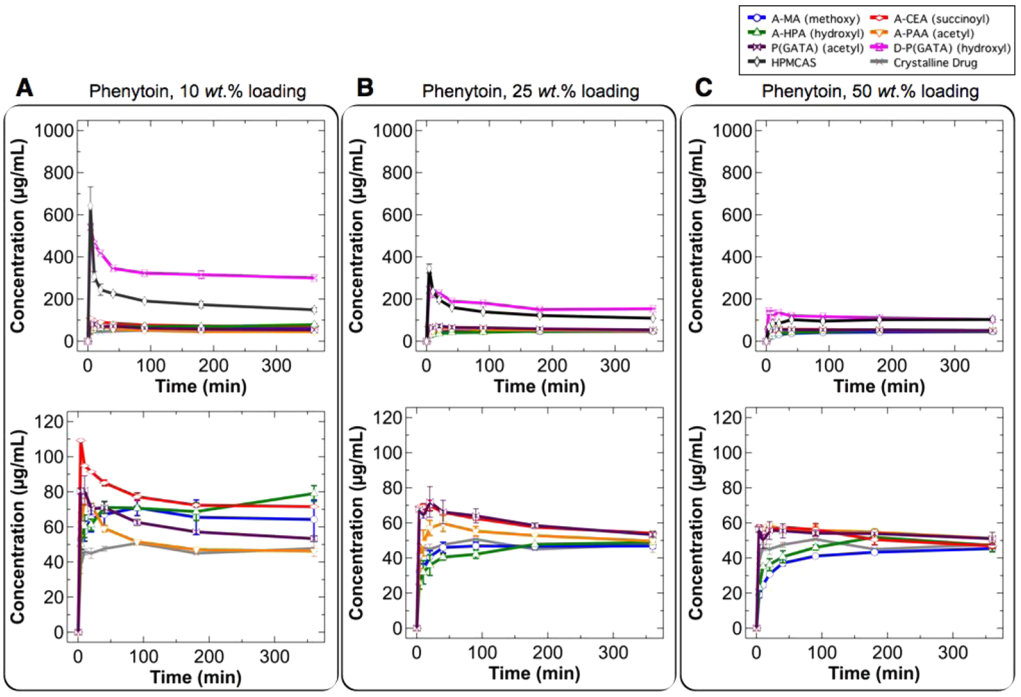

Figure 8. Dissolution tests of phenytoin-loaded systems with A-MA (blue circle), A-CEA (red diamond), A-HPA (green triangle), A-PAA (orange inverted triangle), P(GATA) (purple bowtie), D-P(GATA) (pink hourglass), and HPMCAS (black rhombus) at (A) 10 wt % loading, (B) 25 wt % loading, and (C) 50 wt % loading. The dissolution of crystalline drug (gray X) is also shown as a reference. The total drug loading of all experiments is 1000 μg/mL. The top and bottom rows show the full and up-close dissolution profiles, respectively. Error bars denote the range of the measured data.

release and provide repulsive surface coverage to facilitate polymer−drug interactions (e.g., acetyl-hydroxyl hydrogen bonding), overcoming the high lipophilicity of probucol. This type of interaction for probucol was observed in the solid-state by FTIR and likely responsible for maintaining such high levels of supersaturation. However, the extent of whether probucol was truly molecularly dissolved or aggregated is not well understood. Limited drug concentrations in aqueous media and low stability of supersaturated solutions in aqueous settings have traditionally plagued the pursuit of this question. We conducted a 1D ^{1}H NMR study with A-CEA and probucol, but the results were inconclusive (see the Supporting Information).

This amphiphilicity is not present in water-soluble D-P(GATA) SDDs, where the C_{max} remains limited despite the water solubility of the polymer itself. Thus, some hydrophobic (or lipophilic) component is necessary to inhibit probucol precipitation. Furthermore, the more water-insoluble SDDs give slow and limited probucol release, driven by Fickian-like diffusion through the carrier polymer matrix. This is evident in hydrophobic systems A-MA, A-HPA, A-PAA, and P(GATA), where probucol concentrations increase monotonically over time (C_{max} = $C_{360\ min}$) in Figure 6A, B. Selective sugar hydrolysis of A-MA enhanced the dissolution rate of these SDDs at high probucol loadings, showing the importance of polymer hydrophilicity in enabling release (Figure S15). Visually, these particles remained solid throughout the experiment. In Figure 6C, at 50 wt % probucol loading, all systems offer very limited dissolution enhancement over pure probucol because a significant fraction of the probucol had already crystallized, as seen by PXRD in Figure 5. For A-PAA loaded with 50 wt % probucol, we believe that the inconsistent release profile resulted from C_{tot} measurement error due to the extent of phase separation between polymer, amorphous drug, and crystalline drug in the solid-state.

Danazol Dissolution. In comparison to probucol-containing SDDs, the dissolution performance of danazol-loaded systems in Figure 7 is extraordinarily different. Surprisingly, D-P(GATA) outmatched HPMCAS at 10 wt % loading: after achieving an initial burst release to C_{max} = 758 ± 53 μg/mL, amorphous danazol precipitated out of solution and settled at $C_{360\ min}$ = 215 ± 7 μg/mL. Meanwhile, the same qualitative trend can be observed for the amphiliphic A-CEA analog at 10 wt % danazol with C_{max} = 384 ± 0.05 μg/mL and $C_{360\ min}$ = 78 ± 2 μg/mL. Both polymer excipients are able to release danazol immediately, becoming visually clear at initial time points before precipitated solids appeared out of solution at all drug loadings. But a comparison of these $C_{360\ min}$ values suggests that for danazol, hydroxyl functionalities in polymeric excipients play a more vital role in maintaining supersaturation.

On the log P−T_m state space, danazol is less hydrophobic but a stronger crystallizer. Walton et al. used diffractometry and computation to show that danazol exhibited an overall planar shape with intermolecular O(hydroxy)···O(isoxazole) hydrogen bonds in its crystal structure.[32] We hypothesize that pendant hydroxy groups in D-P(GATA) can hydrogen bond to isoxazole groups in danazol, directly interfering with its precipitation/crystallization from solution. The reduction in birefringent crystal size from Figure 3 further supports this notion. Furthermore, Jackson and co-workers studied the precipitation tendency of supersaturated danazol systems in the presence of polyvinylpyrrolidone, hydroxypropyl methyl cellulose, and HPMCAS.[33] They reported that by using ultraviolet and fluorescence spectroscopy above its amorphous solubility, danazol underwent liquid−liquid phase separation into a transient drug-rich phase before crystallization. In this

DOI: 10.1021/acsbiomaterials.5b00234
ACS Biomater. Sci. Eng. XXXX, XXX, XXX−XXX

manner, we believe that D-P(GATA) interacts with danazol in during both phase separation and crystallization processes, enabling the burst release at short times and extending the supersaturation maintenance period to longer times.

All other systems provide minimal improvement over the release of crystallized danazol, which peaked and plateaued at $C_{max} \approx 70$ μg/mL and $C_{360} \approx 30$ μg/mL, respectively. In fact, A-MA completely restricted the initial burst release of amorphized danazol because of its polymer insolubility. A-HPA, A-PAA, and P(GATA) show improved C_{max} values from keeping danazol initially in solution, where the rate of crystallization-induced desupersaturation best inhibited by A-HPA (the hydroxypropyl acrylate analog) for all drug loadings. This again demonstrates that crystallization obstruction by intermolecular hydrogen bonding may be a key parameter to improving oral bioavailability.

Phenytoin Dissolution. The results of the solution-state studies involving phenytoin strongly resemble the dissolution behavior of danazol. Figure 8 shows the dissolution profiles of SDDs at 10, 25, and 50 wt % phenytoin loadings. Again, glycopolymer D-P(GATA) is able to best prevent desupersaturation as a nucleation and crystal growth inhibitor, outperforming even HPMCAS up to 50 wt % loading in terms of the highest $C_{360\ min}$. Polymer hydrophilicity appears particularly important. For example, selectively deprotecting the GATA acetyl groups for A-MA led to a higher achievable C_{max} (Supporting Information). The remaining SDDs exhibited low dissolution performances with $C_{max} \leq C_{360\ min}$. In the literature, the strong crystallization tendency of phenytoin occurs in a rodlike, uniaxial manner that is highly dependent on the surrounding medium conditions.[34] The birefringent PLM images in Figure 3 clearly show this crystal morphology as phenytoin quickly precipitated out of solution. At higher C_{tot} values, the crystals formed are even larger (see the Supporting Information). Thus, understanding the crystallization mechanism of phenytoin is important for solid dispersions because polymer interactions compete with crystallization kinetics.

For phenytoin, this mechanism has been explored. Zipp et al. reported that crystal growth is limited by surface integration rather than mass transport, driven predominately by "ribbons" of hydrogen bonds between amino hydrogen and carbonyl oxygen groups.[35] This phenomenon is prevalent in biological chemistry, where similar hydrogen bonding patterns are responsible for complementary base pairs recognition and folding structure in nucleic acids. We speculate that the polymers with structures capable of interfering with phenytoin's highly directional intramolecular hydrogen bonding growth sites may be key to preventing its desupersaturation from solution. Other phenytoin studies that employ model polymer systems using identical in vitro dissolution testing conditions (C_{tot} = 1000 μg/mL) and procedures support this hypothesis. For instance, Yin et al. studied the dissolution of phenytoin with modified hydroxypropyl methyl cellulose esters and attributed the best nucleation inhibition behavior to systems with a high degree of succinate substitution and cyclohexylthio content for facilitating colloidally stabilized surface coverage.[36] Alternatively, Dalsin et al. confined phenytoin into various micellar N,N-dimethylacrylamide (DMA) and poly(ethylene-*alt*-propylene) (PEP) block polymers before spray drying and observed no apparent solubility enhancement.[37] Here, the formation of micelles or physical nanoaggregates with DMA and PEP constituents would in principle spatially localize phenytoin molecules and impede mass transport. However, because surface integration is likely the rate-limiting step for phenytoin crystallization, no significant advantage was achieved. Finally, recent work by Widanapathirana et al. show that a *N*-isopropylacrylamide (NIPAm) and vinylpyrrolidone (VP) model system was able to release phenytoin-loaded solid dispersions to moderate supersaturation levels without evidence of desupersaturation.[38] They proposed that the structural similarity of NIPAm to phenytoin inhibited crystallization by disrupting the drug's hydrogen bonding mechanism. In short, the results of our work and of similar model systems show that excipients designed to specifically interfere with crystal growth pathways can outperform commercial polymers like HPMCAS. This simple idea can greatly enhance the viability of kinetically binding metastable drug molecules to advance solid dispersions technology for oral drug delivery.

Generalizations for Excipient Design. The oral bioavailability of probucol, danazol, and phenytoin can be quantified in terms of the area under the dissolution curve (AUC_{dis}) of the concentration−time dissolution profiles. To gain a better metric of excipient effectiveness, we can normalize these values by the AUC_{dis} of the pure drug dissolution at C_{tot} = 1000 μg/mL, such that an $AUC_{360\ min}$ enhancement of 10 means a 10-fold increase in the solubilized drug made available for oral delivery by using the SDD vehicle. These $AUC_{360\ min}$ enhancement values are compared in Figure 9. In general, the enhancement factors between our model drugs are distinct. For probucol, over 100 times improvement in the apparent solubilization was demonstrated for excipients like A-CEA and HPMCAS; for danazol and phenytoin, the enhancement is over an order of magnitude smaller. However, because deprotected glycopolymer D-P(GATA) best prolonged precipitation, we gain insight into how future excipient platforms can be rationally designed for fast-crystallizing drugs.

Finally, we conducted dissolution tests of SDDs with the presence of additional polymer additive. The "spring-parachute" concept was coined by Williams et al. to describe the drug release mechanism for solid dispersions.[39] As qualitatively depicted in Figure 1, an amorphous drug "spring" into a supersaturated (high free energy) state upon release into solution, where a polymer "parachute" kinetically extends the gradual return to equilibrium. Our objective was to evaluate this idea to gain a clearer sense of the crystallization kinetics since discriminating the interconnected polymer−drug, polymer−polymer, and drug−drug associations in solution remains complex and experimentally challenging. Figure 10 shows a schematic representation of the dissolution experiments. A-CEA and D-P(GATA) SDDs loaded with 25 or 50 wt % phenytoin were diluted with D-P(GATA) and A-CEA, respectively, so that the effective drug to polymer ratio was 10 to 90 wt %. The C_{tot} was kept at 1000 μg/mL so that dissolution profiles could be directly compared to SDDs at 10 wt % phenytoin.

This comparative experiment reveals the importance of the initial state of a solid dispersion in the context of the spring-parachute analogy. In Figure 11A, no superadditive effect was observed for A-CEA SDDs in the presence of D-P(GATA) polymer. Here, the additional D-P(GATA) polymer was unable to interact with spray-dried phenytoin molecules in the A-CEA matrix on this time scale. The C_{max} and $C_{360\ min}$ values of 25 and 50 wt % A-CEA SDDs were not improved. Conversely, D-P(GATA) SDDs with added A-CEA in Figure 11B show that ionizable succinoyl groups can mediate supersaturation level maintenance. For instance, the 25 wt % D-P(GATA) SDD

DOI: 10.1021/acsbiomaterials.5b00234
ACS Biomater. Sci. Eng. XXXX, XXX, XXX−XXX

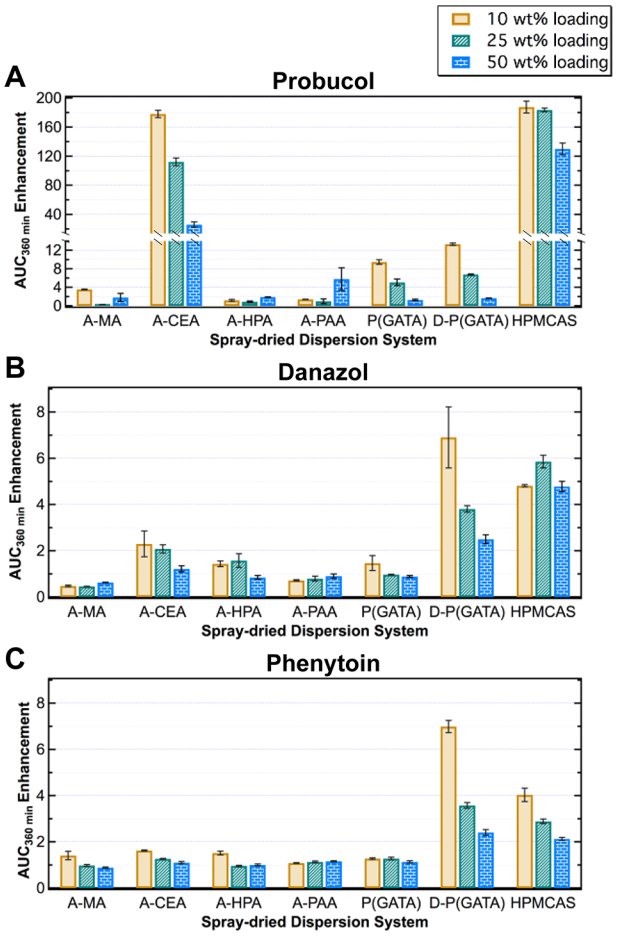

Figure 9. Area under the dissolution curve enhancement over 360 min ($AUC_{360\ min}$ Enhancement) for all investigated spray-dried dispersion systems at 10, 25, and 50 wt % drug loading for (A) probucol, (B) danazol, and (C) phenytoin. Error bars denote the range of the measured data.

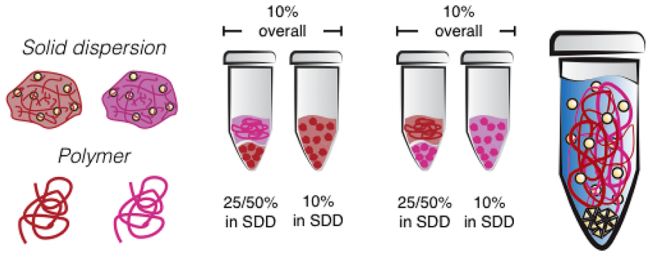

Figure 10. Illustration of dissolution tests containing phenytoin-loaded solid dispersions prepared with either A-CEA (red) or D-P(GATA) (pink) and A-CEA or D-P(GATA) polymer additives. To examine the effects of polymer additives on supersaturation maintenance during drug dissolution, A-CEA polymer was added to D-P(GATA) solid dispersion samples loaded with 25 and 50 wt % phenytoin so that the net drug to polymer loading was effectively 10 wt %. Likewise, D-P(GATA) polymer was combined with A-CEA solid dispersion samples in the same manner. The total targeted drug concentration was kept at C_{tot} = 1000 μg/mL.

achieved a slightly higher $C_{360\ min}$ as the 10 wt % value after 90 min. This suggests that phenytoin molecules are indeed interacting with D-P(GATA) molecules in the SDDs to inhibit phenytoin nucleation and crystal growth. The presence of an amphiphilic, ionizing polymer enhanced its stabilization over

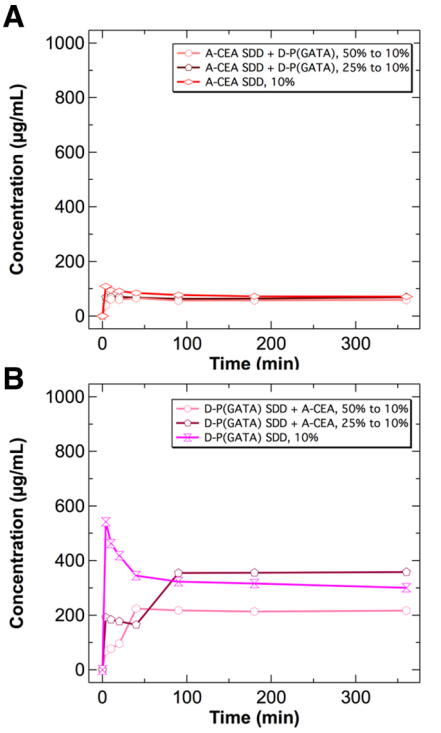

Figure 11. Dissolution tests of 10 wt % phenytoin-loaded systems with (A) A-CEA SDDs (red diamond) and (B) D-P(GATA) SDDs (pink hourglass), compared to combinatorial dissolution experiments. In these experiments, the effective total phenytoin concentration was reduced to 10 wt % for the 50 and 25 wt % A-CEA SDDs with D-P(GATA) (light red pentagon and dark red hexagon, respectively), as well as the 50 and 25 wt % D-P(GATA) SDDs with A-CEA (light pink pentagon and dark pink hexagon, respectively).

longer time scales. In the context of the spring-parachute analog, a fast-crystallizing drug needs the polymer parachute associating with it initially in the spring state. Excipients aimed at stopping the nucleation and crystal growth kinetics directly may augment dissolution performance. We speculate that the inclusion of crystallization-suppressing additives via polymer blending may provide beneficial effects for boosting the oral bioavailability of SDD systems.

CONCLUSIONS

Altogether, we have synthesized a series of acrylic HPMCAS-inspired copolymers to study the complex roles that polymers play as vehicular solubilizing excipients in pharmaceutical formulation and oral drug delivery. This synthetic platform provided a means to decouple the methoxy, hydroxyl, acetyl, and succinoyl substituents of HPMCAS into chemically equivalent monomers and judiciously combine them with RAFT chemistry in a controllable manner over structural parameters. Probucol, danazol, and phenytoin were selected as BCS Class II drugs for spray drying to span the log $P-T_m$ state-space (indicators of intrinsic hydrophobicity and crystallization propensity, respectively). By varying the polymer−drug combinations and loadings, we analyzed the amorphicity of prepared SDDs and conducted in vitro dissolution experiments to measure apparent solubility and investigate the interplay between structure and functionality.

The design of an excipient for solid dispersions is integral toward formulation of highly individualized hydrophobic drug molecules. In particular, lipophilic drugs like probucol that are

DOI: 10.1021/acsbiomaterials.5b00234
ACS Biomater. Sci. Eng. XXXX, XXX, XXX−XXX

susceptible to phase-separation require hydrophobic interactions and polymer−drug complexation. In HPMCAS, this is reflected in the acetyl-succinoyl ratio that drives ionic repulsion and colloidal associations such as hydrophobic−hydrophobic interactions and hydrogen bonding. By comparison, stronger crystallizers such as danazol or phenytoin need excipients that can disrupt nucleation and crystal growth processes to maintain supersaturation levels. The capability of hydroxyl groups in adsorbing onto precipitated danazol and phenytoin crystals was recognized and will remain the subject of more rigorous future work.

With the advancement of tunable platforms to establish mechanistic structure−property relationships, the renewed field of excipient formulation is poised to bring transformative new medicines into clinical applications. For current solid dispersion investigations in oral drug delivery, we foresee challenges in attempting to identify or invent a single, outstanding excipient that is equipped to effectively solubilize a myriad of insoluble compounds with diverse structures and physiochemical attributes. However, incorporating specific noncovalent polymer−drug interactions in universal manners can overcome such limitations and guide strategic development of customized excipients for potential blockbuster drugs in commercial therapeutic products.

EXPERIMENTAL SECTION

Materials. The chemicals below were reagent grade and used as received from Aldrich unless otherwise noted: methyl acrylate (MA, 99%), 2-carboxyethyl acrylate (CEA), 2-hydroxypropyl acrylate (HPA, Polysciences Inc.), 2-propylacetyl acrylate (PAA, prepared from HPA acetylation with 4-dimethylaminopyridine at 0 °C with 200 ppm monomethyl hydroquinone inhibitor) 2,2′-azobis(2-methylpropionitrile) (AIBN, 98%), sodium methoxide (NaOMe, 25 wt % in methanol), Dowex-H^+ resin, probucol, danazol, phenytoin, chloroform-*d* ($CDCl_3$, Cambridge Isotope Laboratories, Inc., 99.8 atom % D + 0.05% V/V TMS), deuterium oxide (D_2O, Cambridge Isotope Laboratories, Inc., 99.9 atom % D), dimethyl sulfoxide-d_6 (DMSO-d_6, Cambridge Isotope Laboratories, Inc., 99.9 atom % D) 3-(trimethylsilyl)propionic-2,2,3,3-d4 acid sodium salt (TSP, 98 atom % D), 4-dimethylaminopyridine (≥99%), diethyl ether (anhydrous, ≥ 99%, Fisher Chemical), acetone (≥99.5%), dichloromethane (anhydrous, ≥ 99.8%), methanol (MeOH, 99.8%), tetrahydrofuran (THF, ≥ 99.9%), dimethyl sulfoxide (DMSO, ≥ 99.9%, Fisher Chemical) and dimethylformamide (DMF, 99.8%).

RAFT chain-transfer agent 4-cyano-4-(propylsulfanylthiocarbonyl) sulfanylpentanoic acid (CPP) was prepared as described by Xu et al.[14] HPMCAS (AFFINISOL 126G) was supplied by The Dow Chemical Company. Phosphate buffered saline (PBS, pH 6.5) solutions for dissolution testing consisted of sodium chloride (82 mM, Fisher, ≥ 99.0%), sodium phosphate dibasic heptahydrate (20 mM, Fisher, 98%), and potassium phosphate monobasic (47 mM, J.T. Baker, ≥ 99.0%). Fasted simulated intestinal fluid powder (FaSSIF, containing 3 mM sodium taurocholate, 0.2 mM lecithin, 34.8 mM sodium hydroxide, 68.62 mM sodium chloride, and 19.12 mM maleic acid) was purchased from Biorelevant (Surrey, UK).

Monomer and Polymer Syntheses. All syntheses were conducted under nitrogen in oven-dried glassware. Inhibitors in MA, CEA, HPA, and PAA were removed with an activated alumina column. PAA was prepared from HPA via acetylation with DMAP at 0 °C with ∼200 ppm monomethyl hydroquinone inhibitor. Glycomonomer GATA was synthesized as described in a published procedure.[21] Pairwise reactivity ratios for these acrylic monomers were taken from our previous work.[17] RAFT polymerizations were performed in a dry 50 mL round-bottom flask containing monomers, initiator, chain transfer agent, and DMF. The solution was sealed and degassed under nitrogen at room temperature for 30 min before transfer into a preheated, well-mixed oil bath at 70 °C. The reaction progress was observed by taking periodic aliquots for ^{1}H NMR. Upon near completion in ∼24 h, polymerizations were quenched into an ice bath and exposing the flask to air. Three rounds of precipitation into diethyl ether with minimal dichloromethane were conducted to remove DMF and residual monomer. Subsequently, precipitated sample was filtered, washed, and dried under a vacuum for 12 h before characterization.

Deprotection chemistry for the glycopolymer P(GATA) to form D-P(GATA) was conducted according to our previous work.[15] More details are provided there. In summary, NaOMe was added dropwise to P(GATA), predissolved in a dry MeOH/$CHCl_3$ mixture (2:1, *v*/*v*), until a pH 9 was reached. After 30 min, the reaction was quenched with Dowex-H^+ resin and water. The complete disappearance of sugar acetate peak at 2.10 ppm by proton nuclear magnetic resonance (^{1}H NMR) confirmed the completion of reaction. D-P(GATA) was further dried under vacuum overnight for 12 h.

Polymer Characterization and Instrumentation. Polymer molecular weights and chemical compositions were analyzed by size exclusion chromatography (SEC) and ^{1}H NMR spectroscopy, respectively. SEC experiments were run on an Agilent 1260 Infinity liquid chromatogram equipped with one Waters Styragel guard column and three Waters Stryragel columns (HR6, HR4, and HR1) with pore sizes suitable for materials (100−10,000,000 g/mol). THF was run as the mobile phase at 1.0 mL/min at 25 °C. The SEC instrument used a Wyatt Dawn Heleos II multiangle laser light scattering (MALS) detector at a laser wavelength of 663.6 nm (18 angles from 10° to 160°) and a Wyatt Optilab T-rEX refractive index detector operating at 658 nm. The d*n*/d*c* values were measured with an Abbe Refractometer equipped with a red light-emitting diode and were used to calculated the absolute molecular weight and dispersity of all polymers using ASTRA 6 software. ^{1}H NMR measurements were performed using a Varian Inova 500 spectrometer at 22 °C with a 10 s relaxation time and 16 transients to minimize signal-to-noise.

Spray Drying. Spray drying was conducted with a Bend Research Mini Spray Dryer (Bend, OR). A 2 wt % of polymer and drug solution at 10, 25, and 50 wt % drug loading in either acetone or acetone/methanol mixture (1:1, *v*/*v*) was prepared, with the following as an example: 100 mg probucol and 100 mg A-MA polymer were added to 9.8 g acetone to prepare 50 wt % spray-dried dispersions (SDDs) from 2 wt % total solute. The solution was well-mixed for at least 30 min and was transferred to a 20 mL syringe for spray drying with the following parameters: solution feed rate = 0.65 mL/min, inlet temperature = 90 °C, nitrogen feed rate = 12.8 standard liter per minute (SLPM). The outlet temperature varied from 25 to 30 °C. SDDs were carefully removed from the 1.5" Whatman filter paper using an antistatic bar and stored in a vacuum desiccator at 22 °C.

Scanning Electron Microscopy (SEM). SDDs were spread on carbon tape and sputter-coated with a 100 Å conductive gold/palladium coating (60:40, %, *w*/*w*) with a Denton DV-502A High Vacuum Deposition System. SEM images were obtained on a Hitachi S-4700 cold field emission gun SEM equipped with a backscattering detector with Autrata modified YAG (yttrium aluminum garnet, cerium doped) crystal. Images were taken at an accelerating voltage and current of 3.0 kV and 10 uA, respectively.

Particle size distributions were reported with ImageJ 1.47v.[40] The longest length scale for 40 randomly selected particles was measured as the representative sample population. The gold/palladium coating thickness (∼100 Å) was subtracted from the particle diameters. Representative histograms were plotted using JMP 9.0.1v.[41]

Powder X-ray Diffraction (PXRD). PXRD experiments were conducted using a Bruker-AXS (Siemens) D5005 Diffractometer with 2.2 kW sealed Cu (λ = 1.54 Å) source, equipped with a scintillation counter detector. SDD samples (50 mg) were placed into standard glass holders. Measurements were taken at a voltage and current of 40 kW and 45 mA, respectively. Samples were analyzed in the 2θ angle range of 5−40° with a step size of 0.02 and scan step time of 0.5 s.

Differential Scanning Calorimetry (DSC), Modulated DSC (MDSC), and Thermogravimetric Analysis (TGA). DSC and MDSC experiments were carried out using a TA Instruments Discovery DSC. All samples (5−10 mg) were hermetically crimped in T-zero aluminum pans. For polymers, second heating experiments

DOI: 10.1021/acsbiomaterials.5b00234
ACS Biomater. Sci. Eng. XXXX, XXX, XXX−XXX

with DSC were conducted from −80 to 180 °C. For SDDs, first heating experiments with MDSC were performed, modulated with ±1 °C amplitude every 40 s from 0 to 150 °C; temperatures were ramped at a rate of 10 °C/min. TA TRIOS software (Version 2.2) was used in the analysis of thermograms. The glass transition temperature (T_g) of all polymers was measured in the second heating scan. The glass transition temperature of SDDs was determined using the reversing thermogram in MDSC during the first heating step. Residual acetone or methanol solvent in spray-dried samples was analyzed by TGA with a Pyris Diamond (PerkinElmer) Thermogravimetric Analyzer model TGA7. Nitrogen was used as a purge gas at a flow rate of 10 mL/min, and a heating rate of 10 °C/min was used for all samples.

Fourier Transform Infrared (FTIR) Spectroscopy. Infrared spectra were collected on a Thermo Scientific Nicolet iS50 FT-IR spectrometer equipped with a built-in diamond attenuated total reflection (ATR) at room temperature in the range of 400−4000 cm^{-1}. The detectors on the main bench and ATR are MCT-A/DLaTGS and DLaTGS, respectively.

Polarized Light Microscopy (PLM). Select polymers were weighed (180 μg) and predissolved in 1 mL phosphate buffer saline (PBS, pH 6.5) solution and filtered through a 0.45 μm syringe filter into 20 mL glass vials. Drugs (1 mg) were dissolved into 1 mL DMSO, and 20 μL (2 vol % DMSO in PBS solution) was introduced to the PBS mixture (effective 10 wt % drug compared to polymer). After 10 min, a small aliquot (10 μL) was transferred onto a glass slide with a coverslip for imaging. All PLM experiments were performed using a Nikon Optiphot polarizing light microscope, equipped with 5×, 10×, 20×, and 50× objectives. The visual bifringence of particles indicated crystallinity. All images were recorded using a Canon SL1 digital camera and processed with a 1% increase in saturated pixels for clarity using ImageJ 1.47v.[39]

Dissolution of Spray-Dried Dispersions (SDDs). Nonsink dissolution tests were carried out using a microcentrifuge dissolution test method. Measured samples (SDDs or crystalline drug) were weighed in duplicates into 2.0 mL plastic conical microcentrifuge tubes. Sufficient volume of PBS solution with 0.5 wt % fasted simulated intestinal fluid powder (FaSSIF) at 37 °C was transferred to each tube, so that a total drug concentration of 1000 μg/mL was established (e.g., 7.2 mg of a A-MA SDD loaded with 25 wt % probucol, consisting of 1.8 mg of drug and 5.4 mg of polymer, was diluted with 1.8 mL PBS/FaSSIF). Samples were briefly vortexed for ∼30 s using a Vortex Genie 2 equipped with a Scientific Industries V524 Vertical Microtube Holder and incubated in a VWR Digital Heatblock at 37 °C until each time point (4, 10, 20, 40, 90, 180, and 360 min). To take an aliquot, samples were first centrifuged for 1 min at 13,000 rpm in an Eppendorf Centrifuge 5414R, followed by transfer of 50 μL from the supernatant and dilution with 250 μL methanol. Finally, samples were vortexed again for ∼30 s to resuspend SDDs and returned to the heating block at 37 °C.

Solublized drug concentrations were measured by reverse phase high-performance liquid chromatography (HPLC). The HPLC contained a reversed-phase EC-C18 column (Poroshell 120, 4.6 × 50 mm, 2.7 μm, Agilent, USA). The mobile phase consisted of acetonitrile/water for probucol (96:4, %, *v/v*), danazol (70:30, %, *v/v*), and phenytoin (60:40, %, *v/v*) at a flow rate of 1.0 mL/min at 30 °C. Each run injected 10 μL of sample, and the column effluent was detected with a UV detector (1260 Infinity Multiple Wavelength Detector, Agilent) at 241 nm for probucol, 284 nm for danazol, and 225 nm for phenytoin. The sample concentrations were determined using a calibration curves ($R^2 > 0.99$, see the Supporting Information). In the dissolution plots, the area under the dissolution curve (AUC_{dis}) from 0 to 360 min was calculated with the trapezoidal rule.

■ ASSOCIATED CONTENT

Supporting Information

The Supporting Information is available free of charge on the ACS Publications website at DOI: 10.1021/acsbiomaterials.5b00234.

Supplemental synthetic procedures; ^{1}H NMR spectra, DSC traces, SEC chromatograms, and d*n*/d*c* refractometry of synthesized polymers; PXRD, MDSC, and FTIR plots of SDDs; drug calibration curves; detailed tabulation of $C_{max}/C_{360\ min}/AUC_{dis}/AUC_{360\ min}$ enhancement for dissolution studies; PLM of high concentrations of crystallized phenytoin (PDF)

■ AUTHOR INFORMATION

Corresponding Authors

* E-mail: bates001@umn.edu. Tel.: 612-624-0839.
*E-mail: treineke@umn.edu. Tel.: 612-624-8042.

Notes

The authors declare no competing financial interest.

■ ACKNOWLEDGMENTS

We acknowledge the financial support of The Dow Chemical Company in this study. We gratefully thank Prof. Marc A. Hillmyer and Prof. Timothy P. Lodge at the University of Minnesota, as well as Dr. Steven J. Guillaudeu, Dr. Robert L. Schmitt, and Dr. William W. Porter III at The Dow Chemical Company, for invaluable discussions and feedback. We also thank Ralm G. Ricarte for assisting with his expertise in SEM imaging, as well as Anatolii A. Purchel and Ziang Li for helpful discussions with FTIR analysis. This material is based upon work supported by the National Science Foundation Graduate Research Fellowship under Grant 00006595. Parts of this work were carried out in the Characterization Facility at the University of Minnesota, a member of the NSF-funded Materials Research Facilities Network (www.mrfn.org) via the MRSEC program.

■ REFERENCES

(1) Lahana, R. Who Wants to Be Irrational? *Drug Discovery Today* **2003**, *8*, 655−656.
(2) Macarron, R. Critical Review of the Role of HTS in Drug Discovery. *Drug Discovery Today* **2006**, *11*, 277−279.
(3) Mullard, A. 2014 FDA Drug Approvals. *Nat. Rev. Drug Discovery* **2015**, *14*, 77−81.
(4) Mitragotri, S.; Burke, P. A.; Langer, R. Overcoming the Challenges in Administering Biopharmaceuticals: Formulation and Delivery Strategies. *Nat. Rev. Drug Discovery* **2014**, *13*, 655−672.
(5) Ma, X.; Zhao, Y. Biomedical Applications of Supramolecular Systems Based on Host−Guest Interactions. *Chem. Rev.* **2015**, *115*, 7794.
(6) Thayer, A. M. Custom Chemicals Go Further. *Chem. Eng. News* **2013**, *91* (6), 10−18.
(7) Kemsley, J. Eyes on Excipients. *Chem. Eng. News* **2014**, *92* (5), 9−11.
(8) Porter, C. J. H.; Trevaskis, N. L.; Charman, W. N. Lipids and Lipid-Based Formulations: Optimizing the Oral Delivery of Lipophilic Drugs. *Nat. Rev. Drug Discovery* **2007**, *6*, 231−248.
(9) Hintz, R. J.; Johnson, K. C. The Effect of Particle Size Distribution on Dissolution Rate and Oral Absorption. *Int. J. Pharm.* **1989**, *51*, 9−17.
(10) Willart, J. F.; Descamps, M. Solid State Amorphization of Pharmaceuticals. *Mol. Pharmaceutics* **2008**, *5*, 905−920.
(11) Hancock, B. C.; Parks, M. What Is the True Solubility Advantage for Amorphous Pharmaceuticals? *Pharm. Res.* **2000**, *17*, 397−404.
(12) Friesen, D. T.; Shanker, R.; Crew, M.; Smithey, D. T.; Curatolo, W. J.; Nightingale, J. A. S. Hydroxypropyl Methylcellulose Acetate Succinate-Based Spray-Dried Dispersions: an Overview. *Mol. Pharmaceutics* **2008**, *5*, 1003−1019.

(13) Curatolo, W.; Nightingale, J. A.; Herbig, S. M. Utility of Hydroxypropylmethylcellulose Acetate Succinate (HPMCAS) for Initiation and Maintenance of Drug Supersaturation in the GI Milieu. *Pharm. Res.* **2009**, *26*, 1419−1431.
(14) Xu, X.; Smith, A. E.; Kirkland, S. E.; McCormick, C. L. Aqueous RAFT Synthesis of pH-Responsive Triblock Copolymer mPEO−PAPMA−PDPAEMA and Formation of Shell Cross-Linked Micelles. *Macromolecules* **2008**, *41*, 8429−8435.
(15) Ting, J. M.; Navale, T. S.; Bates, F. S.; Reineke, T. M. Design of Tunable Multicomponent Polymers as Modular Vehicles to Solubilize Highly Lipophilic Drugs. *Macromolecules* **2014**, *47*, 6554−6565.
(16) Ku, M. S. Use of the Biopharmaceutical Classification System in Early Drug Development. *AAPS J.* **2008**, *10*, 208−212.
(17) Ting, J. M.; Navale, T. S.; Bates, F. S.; Reineke, T. M. Precise Compositional Control and Systematic Preparation of Multimonomeric Statistical Copolymers. *ACS Macro Lett.* **2013**, *2*, 770−774.
(18) Caydamli, Y.; Ding, Y.; Joijode, A.; Li, S.; Shen, J.; Zhu, J.; Tonelli, A. E. Estimating Monomer Sequence Distributions in Tetrapolyacrylates. *Macromolecules* **2015**, *48*, 58−63.
(19) Mayo, F. R.; Lewis, F. M. Copolymerization. I. a Basis for Comparing the Behavior of Monomers in Copolymerization; the Copolymerization of Styrene and Methyl Methacrylate. *J. Am. Chem. Soc.* **1944**, *66*, 1594−1601.
(20) Skeist, I. Copolymerization: the Composition Distribution Curve. *J. Am. Chem. Soc.* **1946**, *68*, 1781−1784.
(21) Mahkam, M. New pH-Sensitive Glycopolymers for Colon-Specific Drug Delivery. *Drug Delivery* **2007**, *14*, 147−153.
(22) Babcock, W. C.; Friesen, D. T.; Nightingale, J. A. S.; Shanker, R. M. Pharmaceutical Solid Dispersions. European Patent EP1 027 886 A2, August 16, 2000.
(23) Vehring, R. Pharmaceutical Particle Engineering via Spray Drying. *Pharm. Res.* **2008**, *25*, 999−1022.
(24) Tetko, I. V.; Gasteiger, J.; Todeschini, R.; Mauri, A.; Livingstone, D.; Ertl, P.; Palyulin, V. A.; Radchenko, E. V.; Zefirov, N. S.; Makarenko, A. S.; Tanchuk, V. Y.; Prokopenko, V. V. Virtual Computational Chemistry Laboratory − Design and Description. *J. Comput.-Aided Mol. Des.* **2005**, *19*, 453−463.
(25) Cal, K.; Sollohub, K. Spray Drying Technique. I: Hardware and Process Parameters. *J. Pharm. Sci.* **2009**, *99*, 575−586.
(26) Thybo, P.; Pedersen, B. L.; Hovgaard, L.; Holm, R.; Müllertz, A. Characterization and Physical Stability of Spray Dried Solid Dispersions of Probucol and PVP-K30. *Pharm. Dev. Technol.* **2008**, *13*, 375−386.
(27) Rumondor, A. C. F.; Wikström, H.; Van Eerdenbrugh, B.; Taylor, L. S. Understanding the tendency of amorphous solid dispersions to undergo amorphous-amorphous phase separation in the presence of absorbed moisture. *AAPS PharmSciTech* **2011**, *12*, 1209−1219.
(28) Qi, S.; Moffat, J. G.; Yang, Z. Early Stage Phase Separation in Pharmaceutical Solid Dispersion Thin Films Under High Humidity: Improved Spatial Understanding Using Probe-Based Thermal and Spectroscopic Nanocharacterization Methods. *Mol. Pharmaceutics* **2013**, *10*, 918−930.
(29) Gao, P.; Shi, Y. Characterization of Supersaturatable Formulations for Improved Absorption of Poorly Soluble Drugs. *AAPS J.* **2012**, *14*, 703−713.
(30) Higashino, H.; Hasegawa, T.; Yamamoto, M.; Matsui, R.; Masaoka, Y.; Kataoka, M.; Sakuma, S.; Yamashita, S. In vitro-in vivo correlation of the effect of supersaturation on the intestinal absorption of BCS Class 2 drugs. *Mol. Pharmaceutics* **2014**, *11*, 746−754.
(31) Schram, C. J.; Beaudoin, S. P.; Taylor, L. S. Impact of Polymer Conformation on the Crystal Growth Inhibition of a Poorly Water-Soluble Drug in Aqueous Solution. *Langmuir* **2015**, *31*, 171−179.
(32) Walton, A. R.; Neidle, S.; Foster, A. B.; Nicholls, D. Structure of an Analogue of the Steroidal Isoxazole Danazol, Ethyl 17-Ethynyl-17-Hydroxy-4-Androsteno[2,3-*D*]Isoxazole-3′-Carboxylate. *Acta Crystallogr., Sect. C: Cryst. Struct. Commun.* **1988**, *44*, 1621−1624.
(33) Jackson, M. J.; Toth, S. J.; Kestur, U. S.; Huang, J.; Qian, F.; Hussain, M. A.; Simpson, G. J.; Taylor, L. S. Impact of Polymers on the Precipitation Behavior of Highly Supersaturated Aqueous Danazol Solutions. *Mol. Pharmaceutics* **2014**, *11*, 3027−3038.
(34) Nokhodchi, A.; Bolourtchian, N.; Dinarvand, R. Crystal Modification of Phenytoin Using Different Solvents and Crystallization Conditions. *Int. J. Pharm.* **2003**, *250*, 85−97.
(35) Zipp, G. L.; Rodriguez-Hornedo, N. Growth Mechanism and Morphology of Phenytoin and Their Relationship with Crystallographic Structure. *J. Phys. D: Appl. Phys.* **1993**, *26*, B48−B55.
(36) Yin, L.; Dalsin, M. C.; Sizovs, A.; Reineke, T. M.; Hillmyer, M. A. Glucose-Functionalized, Serum-Stable Polymeric Micelles From the Combination of Anionic and RAFT Polymerizations. *Macromolecules* **2012**, *45*, 4322−4332.
(37) Dalsin, M. C.; Tale, S.; Reineke, T. M. Solution-State Polymer Assemblies Influence BCS Class II Drug Dissolution and Supersaturation Maintenance. *Biomacromolecules* **2014**, *15*, 500−511.
(38) Widanapathirana, L.; Tale, S.; Reineke, T. M. Dissolution and solubility enhancement of the highly lipophilic drug phenytoin via interaction with poly(N-isopropylacrylamide-co-vinylpyrrolidone) excipients. *Mol. Pharmaceutics* **2015**, *12*, 2537−2543.
(39) Williams, H. D.; Trevaskis, N. L.; Charman, S. A.; Shanker, R. M.; Charman, W. N.; Pouton, C. W.; Porter, C. J. H. Strategies to Address Low Drug Solubility in Discovery and Development. *Pharmacol. Rev.* **2013**, *65*, 315−499.
(40) Schneider, C. A.; Rasband, W. S.; Eliceiri, K. W. NIH Image to ImageJ: 25 Years of Image Analysis. *Nat. Methods* **2012**, *9*, 671−675.
(41) *JMP*, version 9.0.1; SAS Institute: Cary, NC, 1989−2007.

DOI: 10.1021/acsbiomaterials.5b00234
ACS Biomater. Sci. Eng. XXXX, XXX, XXX−XXX